

Article

Reduced DEAF1 function during type 1 diabetes inhibits translation in lymph node stromal cells by suppressing *Eif4g3*

Linda Yip¹, Remi J. Creusot¹, Cara T. Pager², Peter Sarnow², and C. Garrison Fathman^{1,*}

¹ Division of Immunology and Rheumatology, Department of Medicine, Stanford University, Stanford, CA 94305, USA

² Department of Microbiology and Immunology, Stanford University, Stanford, CA 94305, USA

* Correspondence to: C. Garrison Fathman, E-mail: cfathman@stanford.edu

The transcriptional regulator deformed epidermal autoregulatory factor 1 (DEAF1) has been suggested to play a role in maintaining peripheral tolerance by controlling the transcription of peripheral tissue antigen genes in lymph node stromal cells (LNSCs). Here, we demonstrate that DEAF1 also regulates the translation of genes in LNSCs by controlling the transcription of the poorly characterized eukaryotic translation initiation factor 4 gamma 3 (*Eif4g3*) that encodes eIF4GII. *Eif4g3* gene expression was reduced in the pancreatic lymph nodes of *Deaf1*-KO mice, non-obese diabetic mice, and type 1 diabetes patients, where functional *Deaf1* is absent or diminished. Silencing of *Deaf1* reduced *Eif4g3* expression, but increased the expression of *Caspase 3*, a serine protease that degrades eIF4GII. Polysome profiling showed that reduced *Eif4g3* expression in LNSCs resulted in the diminished translation of various genes, including *Anpep*, the gene for aminopeptidase N, an enzyme involved in fine-tuning antigen presentation on major histocompatibility complex (MHC) class II. Together these findings suggest that reduced DEAF1 function, and subsequent loss of *Eif4g3* transcription may affect peripheral tissue antigen (PTA) expression in LNSCs and contribute to the pathology of T1D.

Keywords: DEAF1, *Eif4g3*, translational control, peripheral tolerance, type 1 diabetes

Introduction

Autoimmune diseases result from a breakdown in central and/or peripheral tolerance, when self-reactive T cells that are normally deleted or inactivated escape and mediate destruction of peripheral tissues. During central tolerance, maturing thymocytes interact with medullary thymic epithelial cells (mTECs) that ectopically express an array of peripheral tissue antigens (PTAs) under the transcriptional control of the autoimmune regulator gene (*Aire*) (Anderson et al., 2002). Thymocytes expressing T cell receptors specific for these PTAs are typically deleted. However, some self-reactive T cells escape to the periphery, where they are dealt with by additional ‘peripheral tolerance’ mechanisms.

Our previous work has shown that, in the periphery, the transcriptional regulator deformed epidermal autoregulatory factor 1 (DEAF1) can drive the ectopic expression of genes encoding PTAs in lymph node stromal cells (LNSCs) in a manner analogous to that of AIRE in the thymus, and can control the transcription of hundreds of PTA genes, many that are not regulated by AIRE. In the pancreatic lymph nodes (PLNs), we have shown that DEAF1 regulates ~600 genes (Yip et al., 2009). The ectopic expression of PTA genes in several LNSC subsets have been shown to

mediate the clonal deletion of self-reactive T cells (Lee et al., 2007; Nichols et al., 2007; Gardner et al., 2008; Cohen et al., 2010; Fletcher et al., 2010), and may possibly induce T regulatory cells. These LNSCs can present PTA peptides on major histocompatibility complex molecules, and engage autoreactive PTA-specific CD8⁺ T cells, ultimately leading to their deletion.

The proper expression of *Deaf1* may be essential in the maintenance of peripheral tolerance; diminished DEAF1 function has been linked to the development of autoimmune type 1 diabetes (T1D) (Yip et al., 2009). We have shown that during the progression of T1D, *DEAF1* is alternatively spliced to form a dominant negative variant (*DEAF1-VAR*) in the PLNs of human T1D patients and in non-obese diabetic (NOD) mice after 12 weeks of age (Yip et al., 2009). The PLN tissue is important in the priming of autoreactive T cells (Gagnerault et al., 2002), and the age of 12 weeks is pivotal in the progression of NOD disease, as it marks the beginning of infiltrative/destructive insulinitis and hyperglycemia. The human and mouse *DEAF1-VAR* isoforms are functionally similar. Both isoforms are localized in the cytoplasm, where they have no transcriptional control over gene expression, and both exert a dominant negative effect on the canonical isoform of DEAF1 by binding with and retaining it in the cytoplasm. Overexpression of *DEAF1-VAR* leads to reduced DEAF1 function, and subsequently, reduced expression of various genes including PTA genes (Yip et al., 2009).

Received July 25, 2012. Accepted August 9, 2012.

© The Author (2012). Published by Oxford University Press on behalf of *Journal of Molecular Cell Biology*, IBCB, SIBS, CAS. All rights reserved.

In this study, we show that DEAF1 not only regulates the transcription of genes, but surprisingly also controls the translation of genes in LNSCs by regulating the gene expression of the eukaryotic translation initiation factor *Eif4g3* that encodes eIF4GII, a homolog of the more abundantly expressed eIF4GI. These two isoforms share 46% sequence homology at the amino acid level (Gradi et al., 1998a) and act as the scaffold protein for other translation factors including eIF4E and the poly-A binding protein (PABP), that bind to the 5' cap and poly-A tail of the mRNA strand, respectively. It is thought that the eIF4E-eIF4G-PABP complex circularizes the mRNA and ensures efficient re-initiation of translation by 40S subunits that have been released from 80S ribosomes at the mRNA stop codon.

In mammalian cells, the initiation of translation is a target for controlling gene expression, and the improper expression or inhibition of various initiation factors has been linked to different diseases including diabetes (Kimball et al., 1996; Meric and Hunt, 2002; Abbott and Proud, 2004; Sun et al., 2010). eIF4GI and eIF4GII exhibit complementary actions in various assays *in vitro*, but also appear to mediate different activities (Gradi et al., 1998a). eIF4GII appears to be crucial in re-initiating translation in pre-existing mRNA strands (Castello et al., 2006), and is selectively targeted for degradation at a much later time than eIF4GI in poliovirus-infected cells by viral proteinases (Gradi et al., 1998b). eIF4GII is also preferentially recruited during cell differentiation (Caron et al., 2004), and appears to be essential for the proper translation of distinct mRNA species (Castello et al., 2006; Sun et al., 2010).

Here, we show that DEAF1 regulates the expression of *Eif4g3* transcriptionally, but not *Eif4g1*, and demonstrate that *Eif4g3* is reduced in the PLNs of T1D patients and 12-week-old NOD mice, when functional DEAF1 is reduced. Silencing *Deaf1* resulted in the increased expression of *Caspase3* (*Casp3*), a serine protease that degrades eIF4GII (Marissen et al., 2000). The loss of *Eif4g3*/eIF4GII expression inhibits the translation of various genes including *Anpep*, the gene for aminopeptidase N, an enzyme which trims antigenic peptides loaded on MHC class II molecules (Larsen et al., 1996). This protein is involved in cell surface antigen presentation, and has significant effects on T cell activation and specificity (Larsen et al., 1996). Reduced *Eif4g3* also inhibits the translation of several genes that are involved in neuron growth and migration, and may account for the neural tube closure defects that have previously been observed in *Deaf1*-KO mice (Hahm et al., 2004).

These data demonstrate that the control of PTA expression by DEAF1 is more complex than previously thought, involving both transcriptional and translational control mechanisms. The loss of DEAF1 function during T1D and NOD disease may directly reduce transcription of PTA genes or indirectly inhibit the processing and presentation of PTAs in LNSCs through reduced *Eif4g3* expression. This may affect T cell engagement with LNSCs, and contribute to the escape of self-reactive T cells or prevent the induction of autoantigen-specific regulatory T cells.

Results

Reduced expression of *Eif4g3* in the PLNs of *Deaf1*-KO mice

Microarray analysis was performed to examine genes that were differentially expressed in the PLNs of *Deaf1*-KO mice at various

ages. Each Agilent array contains 41000 probes, with one or more binding to each gene. At 4, 12, and 30 weeks of age, 532, 44, and 236 entities, respectively, were found to be up-regulated by ≥ 2 -fold, and 296, 59, and 361 entities, respectively, were found to be down-regulated by ≥ 2 -fold in the PLNs of *Deaf1*-KO mice compared with age-matched controls (Figure 1A; GEO series accession number: GSE29153). Surprisingly, only four genes, *Eif4g3*, *Ercc4* (excision repair cross-complementing rodent repair deficiency, complementation group 4), *Ncr1* (natural cytotoxicity triggering receptor 1), and *Tmem80* (transmembrane protein 80) were consistently down-regulated across all ages (Figure 1A). We assume that the reduction in *Tmem80*, which overlaps with the *Deaf1* gene on chromosome 7, is likely due to a disruption in the *Tmem80* gene rather than a result of transcriptional regulation by DEAF1.

We focused our attention on *Eif4g3* since it may play a key role in the processing and presentation of PTAs in the PLNs. *Eif4g3* was decreased by 2.3- to 3.8-fold in the PLNs among the eight animals examined, with an average fold change of -3.1 (Figure 1B). qPCR analysis confirmed that *Eif4g3* expression was significantly down-regulated in *Deaf1*-KO animals vs. wild-type (WT) controls (Figure 1C). The diminished expression of *Eif4g3* was not compensated for by a change in *Eif4g1* expression (Figure 1D). eIF4GI (encoded by *Eif4g1*) is a homolog of eIF4GII. Both factors can form the 48S pre-initiation complex by binding to other members of the eIF family, the mRNA strand and small 40S ribosomal subunit (Figure 1E).

Eif4g3 and eIF4G3 expression is reduced in the PLNs of 12-week-old NOD mice and human T1D/auto-antibody-positive patients

Eif4g3 expression was found to correlate with functional *Deaf1* expression. In the PLNs of 12-week-old NOD mice, where *Deaf1* expression is reduced and *Deaf1-Var* expression is increased, *Eif4g3* levels were reduced to $\sim 30\%$ of that seen in diabetes-resistant NOD.B10 congenic controls (Figure 2A and Supplementary Table S1). *Eif4g3* expression was not changed in the NOD PLNs at 4 weeks of age, nor in the NOD spleen and cervical lymph nodes at 12 weeks of age (see Supplementary Figure S1 and Table S1). *Eif4g1* expression was measured to examine if changes in this gene might somehow compensate for reduced *Eif4g3* expression. However, *Eif4g1* levels were not altered in the PLNs of NOD vs. NOD.B10 at any age studied (Figure 2B and Supplementary Figure S1).

To determine if our findings in the NOD mouse translate to human T1D, we measured eIF4G3 and eIF4G1 expression in the PLNs of non-diseased individuals and in the PLNs of T1D and auto-antibody-positive patients where there is significantly higher expression of the alternatively spliced non-functional DEAF1 isoform (Yip et al., 2009) (see Supplementary Table S2 for patient data). Similar to 12-week-old NOD mice, T1D/auto-antibody-positive patients expressed significantly lower levels of eIF4G3 in the PLNs but not the spleen (Figure 2C and Supplementary Figure S1). In the PLNs, eIF4G3 expression was reduced to $\sim 50\%$ of control levels, while eIF4G1 expression was unchanged (Figure 2C and D).

Expression of *Deaf1*, *Eif4g3*, and PTA genes in LNSCs

To examine where *Deaf1* splicing and changes in *Eif4g3* expression occur in the 12-week-old NOD PLNs, the tissue was separated

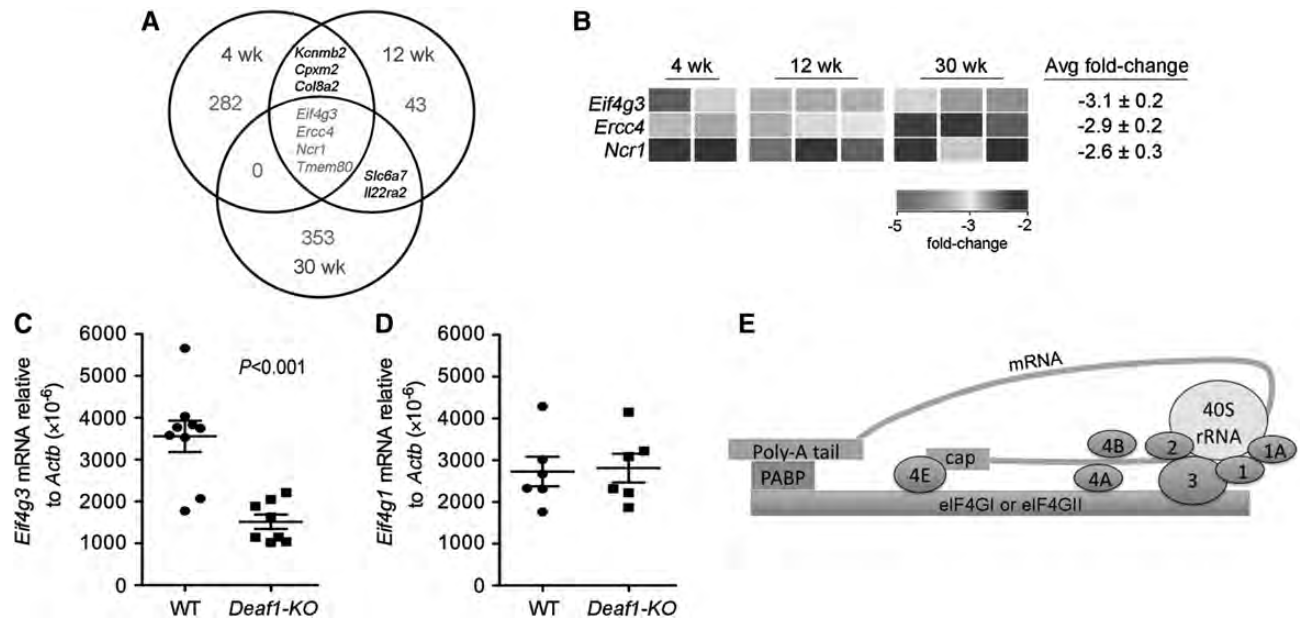


Figure 1 *Eif4g3* gene expression is down-regulated in the PLNs of *Deaf1*-KO mice. **(A)** Venn diagram showing the number of genes down-regulated by ≥ 2 -fold in the PLNs of 4, 12, and 30-week old *Deaf1*-KO mice vs. age-matched controls (4-week old, $n = 2$ per group; 12 and 30-week old, $n = 3$ mice per group), as measured by two-color microarray analysis. Multiple probes for the same gene and unknown genes have been omitted from the regions of overlap. **(B)** Heatmap image showing changes in *Eif4g3*, *Ercc4*, and *Ncr1* gene expression in individual *Deaf1*-KO mice compared with age-matched WT controls. qPCR data showing reduced expression of *Eif4g3* **(C)** and no change in expression of *Eif4g1* **(D)** in the PLNs of *Deaf1*-KO mice compared with littermate controls ($n \geq 6$ mice per group, two-tailed Mann–Whitney test). *Eif4g1* encodes for eIF4GI, a homolog of eIF4GII. **(E)** A schematic diagram showing eIF4GI or eIF4GII in the 48S translation pre-initiation complex. eIF4GI and eIF4GII (encoded by *Eif4g3*) can act as the scaffold for the poly (A)-binding protein (PABP) and other members of the eIF family (shown in blue). The 5' cap and poly-A tail of the mRNA strand (green) binds to eIF4E and PABP, respectively.

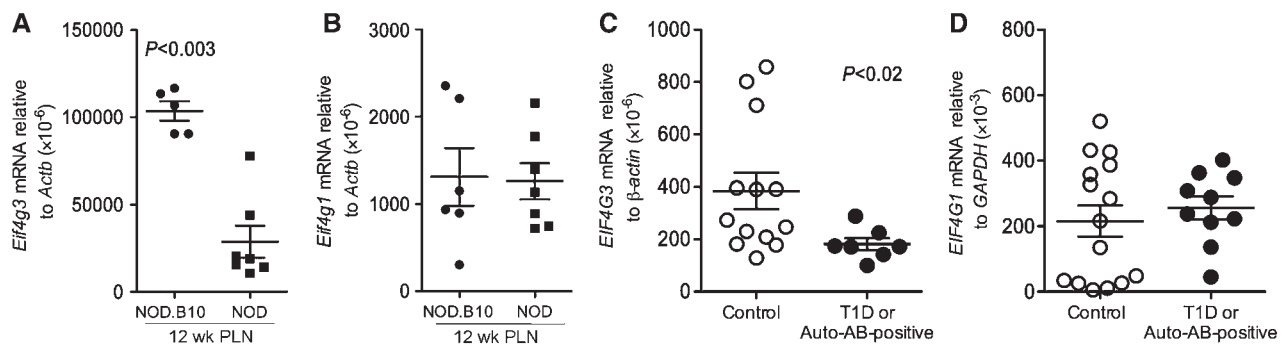


Figure 2 *Eif4g3* mRNA expression is reduced in the PLNs of 12-week-old NOD mice and T1D patients. qPCR data showing reduced *Eif4g3* **(A)** and no change in *Eif4g1* **(B)** expression in the PLN of 12-week-old NOD compared with NOD.B10 mice. qPCR data showing reduced *EIF4G3* expression **(C)** and no change in *EIF4G1* **(D)** expression in the PLNs of T1D/Auto-antibody (AB)-positive patients ($n \geq 7$) compared with non-disease controls ($n \geq 13$). See Supplementary Table S2 for patient information. P -values are indicated on graphs, and determined using the two-tailed Mann–Whitney test. See also Supplementary Figure S1.

into different cellular compartments and *Deaf1*, *Deaf1-Var*, and *Eif4g3* expression was measured. The PLN tissue was initially separated into three major compartments, enriched lymph node stromal elements (LNSE), T cells, and B cells. *Deaf1*, *Deaf1-Var*, and *Eif4g3* gene expression was seen predominantly in the stromal elements of the PLNs (Figure 3A–C). The lymph node stromal elements were further separated into four CD45- subsets based on the expression of gp38 and CD31 as: fibroblastic reticular cells (FRC: gp38⁺, CD31[−]), lymphatic endothelial cells (LEC:

gp38⁺, CD31⁺), blood endothelial cells (BEC: gp38[−], CD31⁺), and double negative cells (DN: gp38[−], CD31[−]) (Figure 3D).

Peripheral lymph nodes of *Deaf1*-WT (BALB/c) mice were pooled, and four LNSE subsets were isolated by fluorescence-activated cell sorting (FACS) (Figure 3D). Three of these subsets (FRC, LEC, and DN) expressed a distinct profile of PTA genes including *Ins2*, *Ambp*, *Fgb*, *Ppy*, *Ela1*, and/or *Tyr* (Figure 3E and Supplementary Table S3). We found that both *Ppy* and *Ins2* were expressed in the LEC and FRC subsets, respectively, as

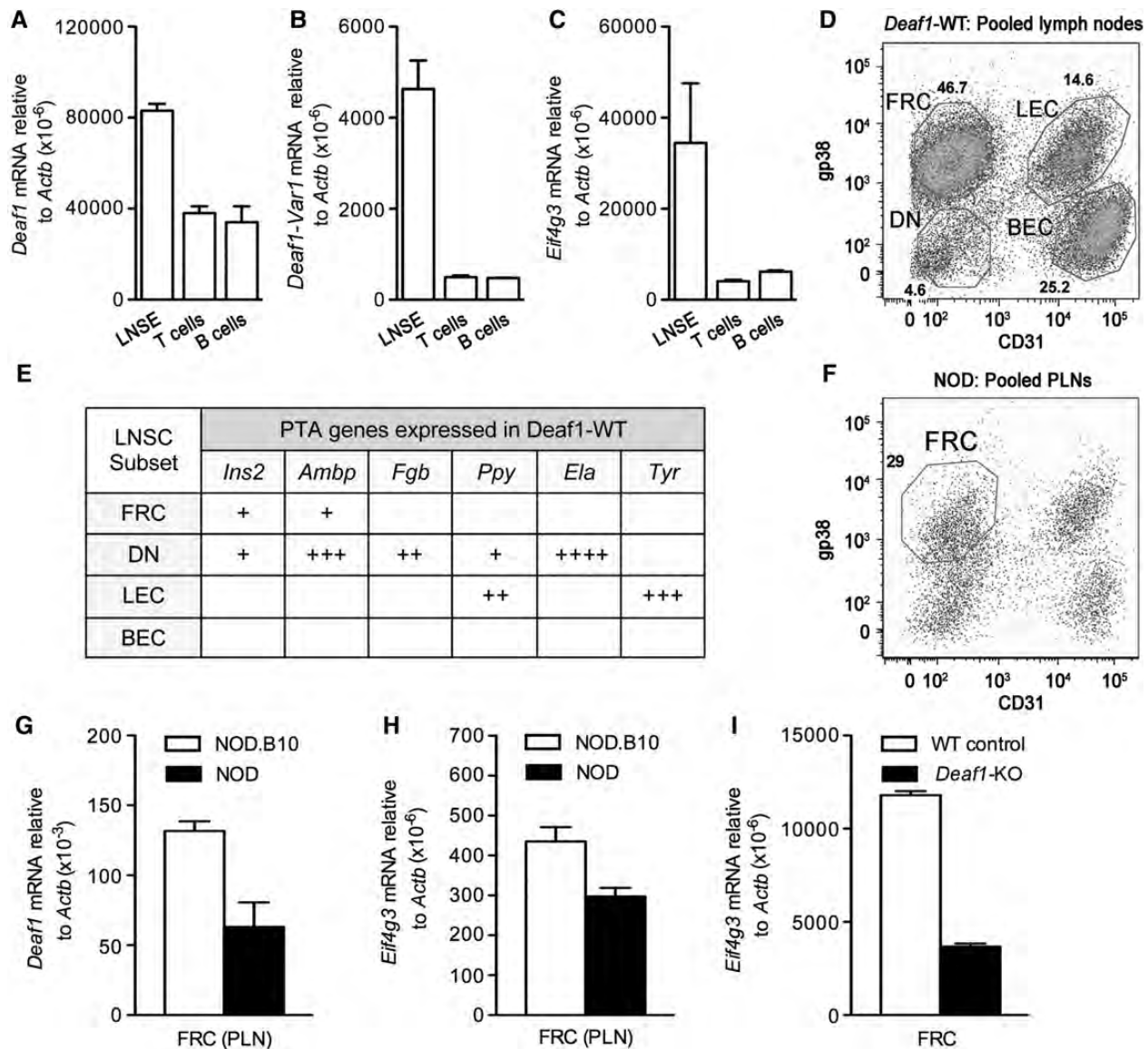


Figure 3 *Deaf1*, *Eif4g3*, and *Ins2* are expressed predominantly in the fibroblastic reticular cell (FRC) subset of LNSCs in the PLNs. qPCR data showing the gene expression of *Deaf1* (A), *Deaf1-Var1* (B), and *Eif4g3* (C) in LNSE, T cells, and B cells isolated from the PLNs of 12-week-old NOD mice ($n = 3$, mean \pm SEM). (D) A representative FACS plot showing the expression of the surface markers, gp38 and CD31, in four distinct cellular subsets of LNSCs (FRC, fibroblastic reticular cells; LEC, lymphatic endothelial cells; DN, double negatives; and BEC, blood endothelial cells) isolated from the pooled lymph nodes (cervical, inguinal, mesenteric, axillary, brachial, and pancreatic lymph nodes) of three *Deaf1*-WT mouse. (E) Each LNSC subset expresses a distinct set of PTA genes, as determined by QPCR. See also Supplementary Tables S3 and S4. (F) A FACS plot showing the FRC, LEC, DN, and BEC isolated from the PLNs of 12-week-old NOD mice (PLNs from 15 individual mice were pooled together). qPCR was performed to measure *Deaf1* (G) and *Eif4g3* (H) gene expression in the FRCs isolated from the PLNs of 12-week-old NOD (pool of 15 individuals) and NOD.B10 (pool of 7–15 individuals) mice, and in FRCs isolated from the pooled lymph nodes of *Deaf1*-KO and WT control mice (pool of three individuals) (I). Data represent the mean \pm SEM of two independent studies.

previously described (Cohen et al., 2010), but in addition, both PTA genes were also expressed in the DN subset. This may be due to strain-specific differences in PTA expression (see Supplementary Table S4), or a difference in the sensitivity of the methods used, as pre-amplification of cDNA was necessary for the detection of both PTA genes by qPCR in the DN subset.

We next examined PTA expression in LNSCs from the PLNs. The four LNSC subsets were isolated from the pooled PLNs of 12-week-old NOD and NOD.B10 mice (Figure 3F). Due to the

low number of cells obtained for each subset, reliable measurement of gene expression was only possible in the most abundant subset, the FRC (up to 7.5×10^4 cells per preparation). Expression levels of both *Deaf1* and *Eif4g3* were lower in the FRCs extracted from the PLNs of 12-week-old NOD compared with those extracted from the NOD.B10 mice (Figure 3G and H). This observation is consistent with the reduced level of *Eif4g3* expression observed in the FRCs extracted from the pooled lymph nodes of *Deaf1*-KO mice compared with WT controls (Figure 3I).

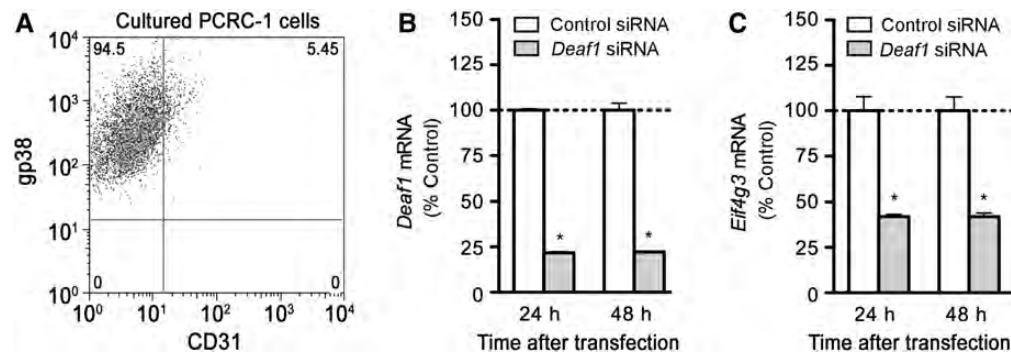


Figure 4 *Deaf1* regulates *Eif4g3* gene expression in immortalized LNSCs. (A) A representative FACS plot showing the expression of gp38, but not CD31 in immortalized LNSCs derived from the pooled lymph nodes of BALB/c mice (PCRC-1). PCRC-1 cells were transfected with control siRNA, or *Deaf1* siRNA and qPCR was performed to measure *Deaf1* (B) and *Eif4g3* (C) gene expression at various times after transfection (mean \pm SEM of three independent experiments, * $P < 0.05$, two-tailed unpaired Student's *t*-test).

To further study the role of *Eif4g3* in PTA expression in LNSCs, we used an immortalized LNSC line, PCRC-1, derived from the pooled lymph nodes of BALB/c mice (Yip et al., 2009). PCRC-1 cells are morphologically and phenotypically similar to primary FRCs (Figure 3D and F), as PCRC-1 cells express gp38 but not CD31 on their surface (Figure 4A), and retain expression of some PTAs like *Ins2*, albeit at lower levels. Using this cell line, we demonstrated that siRNA silencing of *Deaf1* (Figure 4B) led to significantly reduced *Eif4g3* mRNA (Figure 4C), and reduced eIF4G protein expression (Figure 5C). Total eIF4G levels were measured in this study. A specific antibody for mouse eIF4GII is commercially available (Abcam), but we found that it only detected an unspecific product of ~55 kDa when used on PCRC-1 cells.

Down-regulation of *Eif4g3* expression inhibits the translation of various mRNA transcripts in PCRC-1 cells

We next examined the effect of reduced *Eif4g3* expression on gene translation in PCRC-1 cells. Silencing of *Eif4g3* significantly reduced *Eif4g3* and eIF4G expression, without affecting *Eif4g1* levels (Figure 5A–C). Polysomes were isolated from PCRC-1 cells 48 h after transfection with control or *Eif4g3* siRNA, and fractionated into 13 samples of increasing density (Figure 5D). The ribonuclear proteins (RNP) are found primarily in the first two fractions. The top fraction (fractions 3–6) contains the ribosomal subunits, and mRNA strands engaged in pre-initiation complexes. The light polysome fraction (fractions 7–9) contains mRNA transcripts undergoing active translation with few ribosomes attached to each mRNA strand, while the heavy polysome fraction (fractions 10–13) contains mRNA transcripts undergoing translation with multiple ribosomes attached to each mRNA strand.

High-quality RNA was extracted from each fraction (Figure 5E). The 18S rRNA, which makes up the 40S small ribosomal subunit, was detected in fractions 4–5 and 7–13, while the 28S rRNA, which constitutes part of the large ribosomal subunit, was detected in fractions 5–13 (Figure 5E). eIF4G protein was detected only in the RNP and the top fraction, indicating that eIF4GII participates in the early pre-initiation step, but not translational elongation (see Supplementary Figure S2A).

Among the top, light, and heavy fractions of control-siRNA transfected LNSCs, the majority ($92\% \pm 2\%$) of *Eif4g3* mRNA was found in the heavy polysome fraction, where active

translation occurs (see Supplementary Figure S2B). Silencing of *Eif4g3* significantly reduced *Eif4g3* (Figure 5F), but not *Deaf1* levels in the heavy polysome fraction (Figure 5G), while silencing of *Deaf1* reduced both *Eif4g3* (Figure 5F) and *Deaf1* expression in the heavy polysome fraction (Figure 5G). The rate of *Eif4g3* translation, however, was not affected by silencing of *Deaf1*, and the rate of *Deaf1* translation was not affected by silencing *Eif4g3*. This is shown by the similar relative abundance of *Eif4g3* and *Deaf1* mRNA sedimentation in the heavy polysome fraction of *Deaf1*-siRNA or *Eif4g3*-siRNA, and control-siRNA-treated cells (see Supplementary Figure S2C and D).

Microarray analysis was performed to identify genes whose translation is controlled by *Eif4g3*. Gene expression was measured in the heavy fractions and in whole cells lysates 48 h after transfection with *Eif4g3* or control siRNA (GEO Series accession number: GSE39408). Genes with reduced expression in the heavy fraction, but not whole cell lysates, may be controlled by eIF4GII (Figure 5H and Table 1). Genes that are down-regulated in both the whole cell lysates and heavy polysome fractions are not likely controlled by eIF4GII since reduced overall expression of these genes can result in decreased translation in the heavy polysomes (see Supplementary Table S5). Genes that are down-regulated in the whole cell lysate, but not the heavy fraction, may occur as an indirect result of *Eif4g3* silencing (see Supplementary Table S6), for example, by the reduced translation of genes such as *Hcls1*, *Hmgn3*, and *Celf2* that are involved in transcription or pre-mRNA splicing (Table 1 and Supplementary Table S5).

Approximately 22000 entities were detected in the heavy polysome fractions of PCRC-1 cells. Silencing of *Eif4g3* reduced the translation of only 34 of these genes. Eight genes were down-regulated by ≥ 2 -fold in all four individual experiments performed, and 26 genes were down-regulated by ≥ 2 -fold in three of the four experiments performed. Among the eight most consistently down-regulated genes, the top two genes (*Trem1* and *Anpep*) are immune response genes.

Anpep encodes aminopeptidase N (ANP, CD13), an enzyme that fine-tunes antigen presentation on MHC class II molecules by cleaving amino-terminal peptides protruding from MHC class II molecules (Larsen et al., 1996). Reduced DEAF1 function,

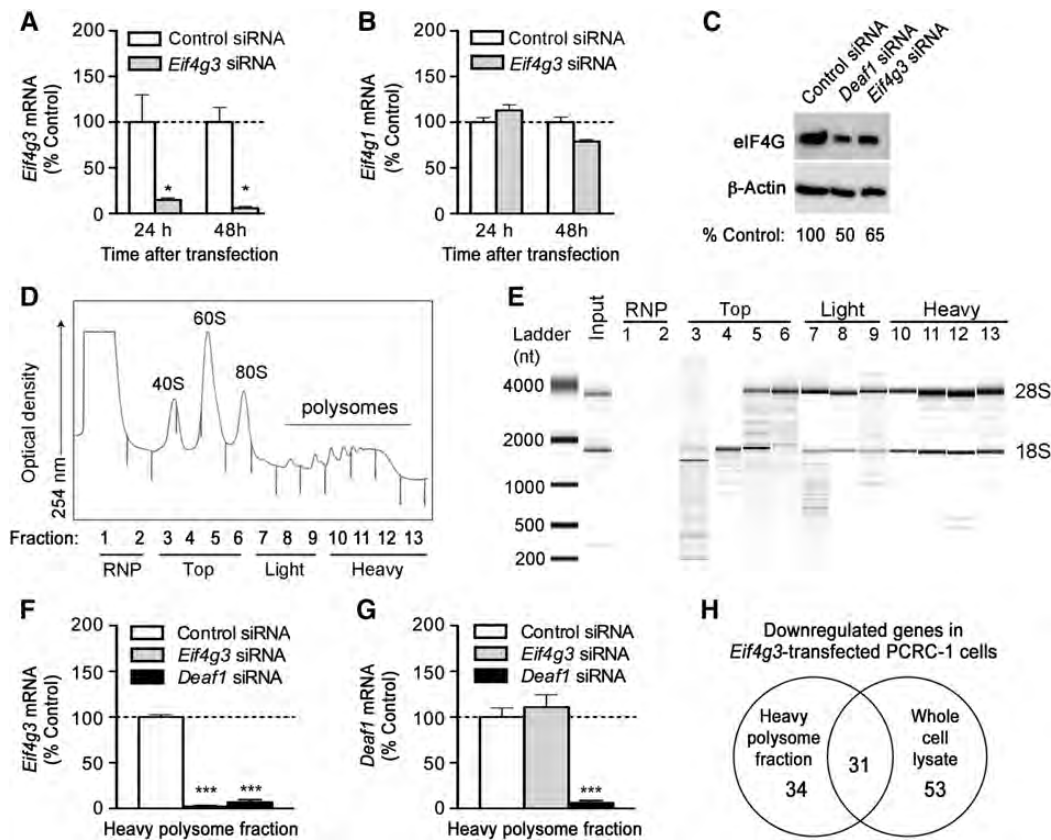


Figure 5 Polysome analysis of *Eif4g3*-silenced PCRC-1 cells. (A and B) PCRC-1 cells were treated with control or *Eif4g3* siRNA, and qPCR was performed to measure *Eif4g3* and *Eif4g1* mRNA expression at various times after transfection (mean \pm SEM of three independent experiments, * $P < 0.05$, two-tailed unpaired Student's *t*-test). (C) Representative immunoblots showing eIF4G and β -actin (loading control) expression 48 h after transfection with control, *Deaf1*, or *Eif4g3* siRNA. (D) Polysomes were isolated from PCRC-1 cells, and 13 fractions of increasing density were collected. These contain the RNP (fractions 1–2), top fractions (fractions 3–6), light polysome fraction (fractions 7–9), and heavy polysome fraction (fractions 10–13). The optical density of each fraction isolated from control siRNA-treated cells, 48 h after transfection, is shown. (E) A representative bioanalyzer gel image showing the RNA extracted from each fraction collected from control siRNA-treated cells, 48 h after transfection. The 18S and 28S rRNA bands are indicated. (F and G) qPCR measurements of *Eif4g3* and *Deaf1* gene expression in the heavy polysome fractions. RNA samples were isolated from fractions collected 48 h after siRNA transfection, and fractions 10–13 were pooled prior to qPCR analysis. Data represent the mean \pm SEM of three independent experiments (*** $P < 0.0005$, two-tailed unpaired Student's *t*-test). Data shown in C–E are representative of three independent experiments. See also Supplementary Figure S2. (H) Venn diagram showing the number of genes that are down-regulated by ≥ 2 -fold in the heavy polysome fraction and total cell lysate of *Eif4g3*-silenced PCRC-1 cells vs. control-siRNA-treated controls, as measured by two-color microarray analysis. Only genes that were reduced by ≥ 2 -fold in at least three out of four individual experiments are included.

diminished *Eif4g3* expression, and subsequent loss of *Anpep* translation could therefore negatively impact antigen presentation by LNSCs.

Reduced translation of genes such as *Slit2*, *Sema5a*, and *Dcl1* that are involved in neuronal migration were also observed after *Eif4g3* silencing. These changes may account for the neural tube closure defects that have previously been observed in $\sim 80\%$ of *Deaf1*-KO mice (Hahm et al., 2004).

Deaf1 regulates *Casp3* expression

eIF4GII is readily cleaved by CASP3 (Marissen et al., 2000). *Casp3* expression was elevated in the PLNs of *Deaf1*-KO mice, 12-week-old NOD mice, and T1D/auto-antibody-positive patients compared with the appropriate controls (Figure 6A–C). Thus, we asked whether DEAF1 might also control eIF4GII expression by regulating the expression of *Casp3*. *Casp3* expression was

found to be significantly higher in samples with absent or diminished DEAF1 function. However, *Casp3* expression was not changed in the PLNs of 4-week-old NOD mice and in the spleen and cervical lymph nodes of 12-week-old NOD mice compared with controls (see Supplementary Figure S3). To examine if reduced *Deaf1* expression led to increased *Casp3* levels in LNSCs, siRNA silencing experiments were performed on PCRC-1 cells. Silencing of *Deaf1* significantly increased *Casp3* expression within 18 h of transfection, without affecting *Casp1* levels (Figure 6D–F). CASP3 protein expression was also significantly increased 18, 24, and 48 h after silencing of *Deaf1* in LNSCs (Figure 6G). Polysome analysis and qPCR demonstrated that the translation of *Casp3* was significantly increased, and functional assays demonstrated increased CASP3 activity after silencing *Deaf1* (Figure 6H and I).

Table 1 Genes that are down-regulated in the heavy polysome fraction but not whole cell lysate of *Eif4g3*-silenced PCRC-1 cells.

Gene symbol	Average fold change (n = 4)	Gene description
Genes down-regulated by ≥ 2-fold in 4 out of 4 separate experiments performed		
<i>Trem1</i>	3.4	Triggering receptor expressed on myeloid cells-like 1
<i>Anpep</i>	3.2	Alanyl (membrane) aminopeptidase, CD13, Aminopeptidase N
<i>Syt13</i>	3.0	Synaptotagmin XIII
<i>Grtp1</i>	2.8	GH regulated TBC protein 1
<i>Ttc39b</i>	2.8	Tetratricopeptide repeat domain 39B
<i>Hcls1</i>	2.7	Hematopoietic cell-specific Lyn substrate 1
<i>Neurl4</i>	2.7	Neuralized homolog 4
<i>Dennd5b</i>	2.6	DENN/MADD domain containing 5B
Genes down-regulated by ≥ 2-fold in 3 out of 4 separate experiments performed		
<i>Mmp3</i>	3.4	Matrix metalloproteinase
<i>Fam71e1</i>	3.1	Family with sequence similarity 71, member E1
<i>Trem2</i>	3.0	Triggering receptor expressed on myeloid cells 2
<i>Fetub</i>	2.7	Fetuin beta (Fetub), transcript variant 1
<i>Pcdh9</i>	2.7	Protocadherin 9 isoform 1
<i>Myom2</i>	2.7	Myomesin 2
<i>Enpp2</i>	2.5	Ectonucleotide pyrophosphatase/phosphodiesterase 2
<i>Acacb</i>	2.5	Acetyl-Coenzyme A carboxylase beta
<i>Abat</i>	2.5	4-aminobutyrate aminotransferase
<i>Slc38a9</i>	2.5	Solute carrier family 38, member 9
<i>Col11a2</i>	2.5	Collagen, type XI, alpha 2
<i>Lgi2</i>	2.5	Leucine-rich repeat LGI family, member 2
<i>Hkdc1</i>	2.4	Hexokinase domain containing 1
<i>Sema5a</i>	2.3	Semaphorin 5A
<i>Tmem87a</i>	2.3	Transmembrane protein 87A
<i>Ctps2</i>	2.3	Cytidine 5'-triphosphate synthase 2
<i>Mudeng</i>	2.2	MU-2/AP1M2 domain containing, death-inducing
<i>Mogat2</i>	2.2	Monoacylglycerol O-acyltransferase 2
<i>Rassf5</i>	2.2	Ras association (RalGDS/AF-6) domain family member 5
<i>Slit2</i>	2.1	Slit homolog 2
<i>Msln</i>	2.1	Mesothelin
<i>Erp44</i>	2.1	Endoplasmic reticulum protein 44
<i>Znf512b</i>	2.0	Zinc finger protein 512B
<i>Lrrk2</i>	2.0	Leucine-rich repeat kinase 2
<i>Sap25</i>	1.9	Sin3 associated polypeptide
<i>Tcp11l2</i>	1.8	T-complex 11 (mouse) like 2

Discussion

Autoimmune diseases, such as T1D, can develop from a breakdown in peripheral tolerance that is partly controlled by PTA gene expression in particular LNSC populations (Gardner et al., 2008; Cohen et al., 2010; Fletcher et al., 2010). We have previously shown that DEAF1 controls the transcription of various genes including some PTA genes in peripheral lymphoid tissues (Yip et al., 2009). Here we demonstrate that DEAF1 also regulates the translation of genes by controlling the expression of *Eif4g3* that encodes eIF4GII. eIF4GII comprises part of the pre-initiation complex that is essential for the initiation of translation (Gingras et al., 1999). We demonstrated that the loss of *Eif4g3*/eIF4GII expression led to reduced translation of various genes including *Anpep*, a gene involved in fine-tuning antigenic peptide presentation on MHC class II molecules. We also showed that silencing of *Deaf1* up-regulated the expression of CASP3, a protease that rapidly degrades eIF4GII (Marissen et al., 2000).

Together, these findings suggest that reduced DEAF1 function during NOD disease or T1D may lead to reduced antigen presentation on LNSCs through diminished PTA and *Eif4g3* gene transcription.

Alternative splicing of *Deaf1* results in the formation of a dominant negative isoform of *Deaf1* (*Deaf1-Var*) that inhibits canonical DEAF1 activity and PTA gene transcription in the PLNs of T1D patients and of 12-week-old NOD mice (Yip et al., 2009). Here, we show that *Eif4g3* expression is also reduced in these tissues, but is not changed in tissues where DEAF1 function is not compromised, such as the spleen of T1D patients and 12-week-old NOD mice, and the PLNs of 4-week-old NOD mice. The loss of DEAF1 function correlates strongly with reduced *Eif4g3* expression, and siRNA silencing experiments suggest that DEAF1 may directly control *Eif4g3* transcription. The precise mechanism is unclear, since DEAF1 does not function as a conventional transcription factor that binds to promoter regions to induce or repress gene expression (Huggenvik et al., 1998). However, the *Eif4g3* gene contains 10 TTCG and 2 TTCCG motifs. These motifs are distributed throughout the gene, and may act as binding sites for DEAF1 (Michelson et al., 1999). Upon binding, DEAF1 may interact with other cell-specific proteins and co-factors to initiate gene transcription (Huggenvik et al., 1998). Alternatively, DEAF1 may regulate *Eif4g3* mRNA abundance at a post-transcriptional step. Interestingly, DEAF1 does not appear to regulate the expression of *Eif4g1*, which encodes eIF4GI, the more abundant isoform of eIF4G.

The presence of two eIF4G homologs has been conserved throughout evolution. In mammals, eIF4GI and eIF4GII have similar biochemical properties and were initially proposed to be functionally redundant (Gradi et al., 1998a). However, translation of *de novo* synthesized mRNA was shown to be highly selective for eIF4GI, while translation of pre-existing mRNA transcripts, or ongoing translation, was found to rely heavily on eIF4GII. Certain mRNA transcripts such as heat shock protein 70 and heat shock chaperone protein HSPA2 are also selective for eIF4GII (Castello et al., 2006; Sun et al., 2010). eIF4GII plays a role in spermatogenesis and mammalian cell differentiation (Caron et al., 2004; Sun et al., 2010), and appears to regulate male germ cell differentiation and meiotic division in *Drosophila* (Baker and Fuller, 2007). In contrast, the two eIF4G isoforms in yeast, eIF4G1 and eIF4G2, were found to compensate for each other, and were not selectively recruited by any particular mRNA transcript (Clarkson et al., 2010).

These studies suggest that multicellular organisms may have evolved to use eIF4GII rather than eIF4GI to regulate translation of specific genes, or for translation in specific cell types such as spermatocytes or LNSCs. LNSCs were historically thought of as the parenchymal support network in lymph nodes, but are now recognized to contain highly specialized cells that constitutively and ectopically express PTAs to induce tolerance of autoreactive T cells that recognize these antigens (Fletcher et al., 2011). To date, several LNSC subsets, the FRC, LEC, BEC, and residual double negative cells (DN) that include the extra-thymic *Aire*-expressing cells (eTACs) have been characterized and found to express a distinct panel of PTAs (Figure 3E) (Gardner et al., 2008; Cohen et al., 2010; Fletcher et al., 2011). Three of these

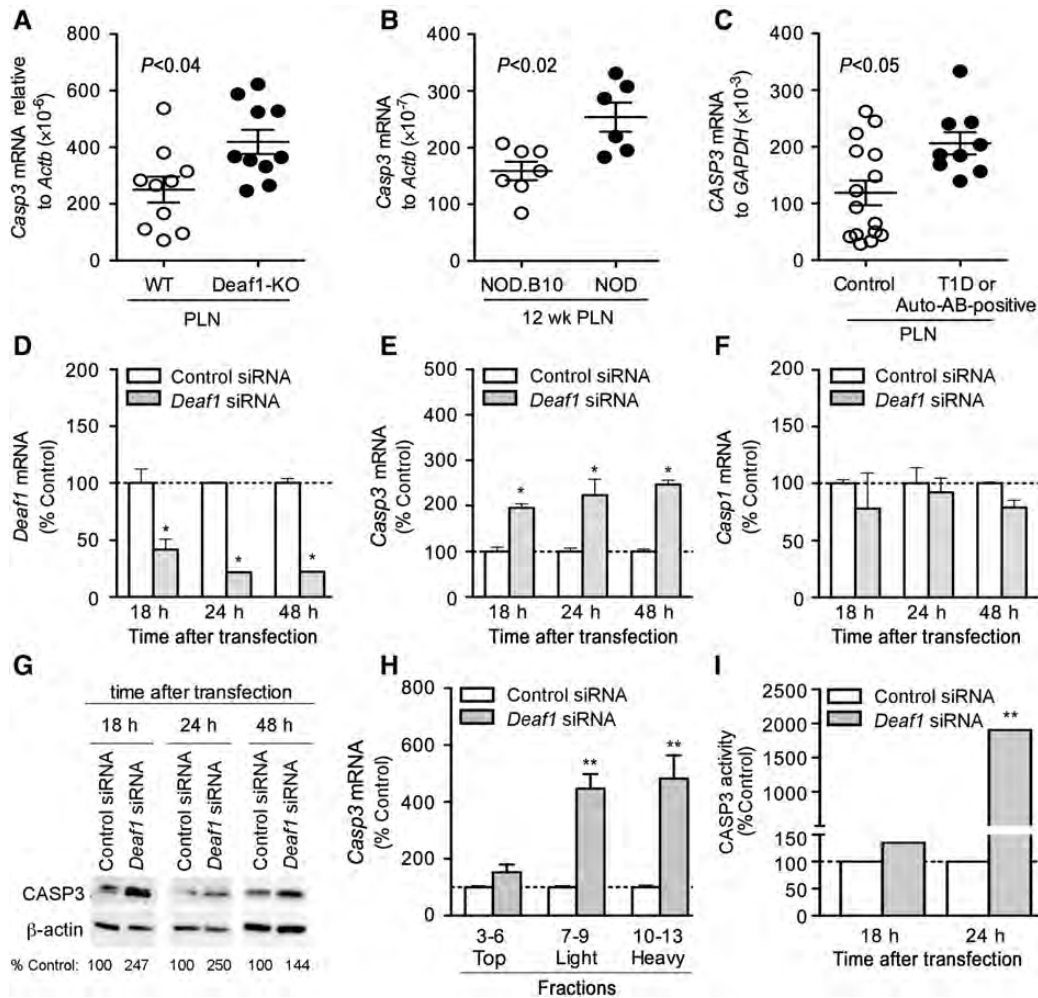


Figure 6 *Deaf1* regulates *Casp3* expression in PCRC-1 cells. qPCR analysis showing up-regulated *Casp3* (A and B) and *CASP3* (C) mRNA expression in the PLNs of *Deaf1*-KO mice vs. littermate controls (A), 12-week-old NOD mice vs. age-matched NOD.B10 controls (B), and T1D/auto-antibody-positive patients compared with non-disease controls (C). *P*-values are indicated on graphs and determined using the two-tailed Mann–Whitney test. PCRC-1 cells were transfected with control or *Deaf1* siRNA and QPCR was performed to measure *Deaf1* (D), *Casp3* (E) and *Casp1* (F) expression at various times after transfection (mean \pm SEM of three independent experiments, * $P < 0.05$, two-tailed unpaired Student's *t*-test). (G) Representative immunoblots showing CASP3 and β -actin (loading control) expression in PCRC-1 cells, 18, 24, and 48 h after transfection with control or *Deaf1* siRNA. Low amounts of CASP3 expression were also observed in untransfected and mock-transfected cells (Supplementary Figure S3D). (H) qPCR analysis of *Casp3* expression in various polysome fractions isolated from PCRC-1 that were transfected with control or *Deaf1* siRNA. RNA samples were collected 48 h after transfection, and pooled as indicated prior to qPCR analysis. Data represent the mean \pm SEM of three independent experiments (** $P < 0.005$, two-tailed unpaired Student's *t*-test). (I) CASP3 activity measured in PCRC-1 cells at various times after transfection with control or *Deaf1* siRNA (mean \pm SEM of three independent experiments, ** $P < 0.005$, two-tailed unpaired Student's *t*-test). See also Supplementary Figure S3.

subsets, the FRC, LEC, and eTACs, were shown to present antigen directly to CD8⁺ T cells that led to the activation and then subsequent deletion of these T cells (Lee et al., 2007; Nichols et al., 2007; Gardner et al., 2008).

In this study, we focused mainly on the FRC subset, the most abundant LNSC subset in the NOD and NOD.B10 PLNs that express MHC class II. They form the mesenchymal network that allows for efficient migration and interaction of T cells, B cells, and dendritic cells. FRCs help arrange the lymph node into distinct regions of T cell zones and B cell follicles (Fletcher et al., 2011). FRCs also exhibit some degree of plasticity, being able to remodel their network within the lymph node upon lymphocyte activation (Katakai et al., 2004). We showed that the expression

of *Deaf1* and *Eif4g3* were markedly reduced in the FRCs derived from the PLNs of 12-week-old NOD mice compared with NOD.B10 controls. Silencing of *Deaf1* in an immortalized FRC-like cell (PCRC-1) resulted in reduced *Eif4g3* gene and eIF4G protein expression. Due to a lack of a suitable antibody, we were only able to measure total eIF4G expression. However, reduced total eIF4G protein is likely due to the loss of eIF4GII expression rather than eIF4GI expression since *Eif4g1* mRNA levels were unchanged by silencing of *Deaf1*.

To examine whether the translation of certain mRNA transcripts are affected by reduced *Eif4g3* expression, we performed polysome analysis after silencing *Eif4g3* in the PCRC-1 cells. Gene expression was measured in the heavy polysome fraction where the

majority of active translation occurs. Surprisingly, more than 22000 entities were detected in this fraction, supporting the notion that LNSCs are able to transcribe and process a vast array of PTA genes. We have observed that cultured PCRC-1 cells can lose the ability to express certain PTAs such as *Ins2*. Thus, primary FRCs may express an even wider range of PTAs than PCRC-1 cells. Silencing of *Eif4g3* reduced the translation of 50 genes including *Anpep*, the gene for aminopeptidase N (CD13). Aminopeptidase N is expressed on antigen-presenting cells including B cells, macrophages, dendritic cells, and lymphoid organs such as lymph nodes, thymus, and spleen (Leenen et al., 1992; Hansen et al., 1993; Gabrilovac et al., 2011). It is expressed with MHC class II (Hansen et al., 1993) and functions to cleave the amino terminal end of antigen peptides bound to MHC class II, thus, altering the final T cell epitope (Larsen et al., 1996). Surface antigen processing by aminopeptidase N has been shown to dramatically affect T cell antigen recognition, T cell activation, and specificity (Larsen et al., 1996). Reduced aminopeptidase N expression due to diminished *Eif4g3* expression, therefore, could affect the presentation of PTAs on LNSCs.

Silencing of *Eif4g3* also reduced the translation of *Slit2*, *Sema5a*, and *Dclk1*, genes that are involved in axonal navigation (*Slit2*, *Sema5a*, and *Dclk1*). These genes may be expressed and presented as PTAs on LNSCs, but in the *Deaf1*-KO mice, reduced translation of these genes during development could account for the exencephaly and neural tube closure defect that affect ~80% of *Deaf1*-KO mouse embryos (Hahm et al., 2004). *Slit2* has been identified as a candidate gene in neural tube defects (Lynch, 2005). This gene is required for proper development of major forebrain tracts, is involved in axonal migration at the ventral midline of the neural tube, and inhibits inappropriate midline crossing by axons (Bagri et al., 2002).

We showed that the loss of DEAF1 function occurs with an up-regulation of CASP3 expression in the PLNs. Previous studies, using CASP3 knockout mice, have shown that CASP3 is required to initiate multiple-low-dose streptozotocin-induced autoimmune diabetes, and that CASP3 knockout mice do not develop diabetes, or show lymphocyte infiltration into the islets in this model (Liadis et al., 2005). Here, we propose that the up-regulation of *Casp3* observed in the PLNs of 12-week-old NOD mice and T1D patients may contribute to diabetes by reducing eIF4GII expression in LNSCs. CASP3 can cleave eIF4G and eIF4GII. The cleavage sites on eIFGII and eIF4GI differ. eIF4GI is cleaved into three products, but maintains an intact core domain that may still retain some function. eIF4GII is cleaved into at least five fragments, and its core central domain is destroyed (Marissen et al., 2000). It is yet unclear whether CASP3 cleaves both isoforms of eIF4G in LNSCs. The up-regulation of CASP3 and degradation of eIF4G is normally associated with cell apoptosis (Marissen and Lloyd, 1998; Marissen et al., 2000). However, silencing of *Eif4g3* and *Deaf1* did not affect LNSCs survival, and did not appear to disrupt the translational machinery. Cell proliferation was not altered after *Deaf1* or *Eif4g3* silencing. In addition, the rate of *Deaf1* and *Eif4g3* translation was not changed in *Eif4g3*-silenced and *Deaf1*-silenced LNSCs, respectively, compared with control cells. Similar findings in yeast show that the loss of eIF4G2 also does not affect cell

proliferation, while the loss of eIF4G1 inhibits cell growth and global translation initiation rates (Clarkson et al., 2010). HeLa cells that were depleted of eIF4GI also showed reduced overall translation and altered cell morphology (Coldwell and Morley, 2006). In accordance with these studies, it is possible that, in LNSCs, eIF4GI, rather than eIF4GII, is preferentially recruited for the translation of genes that are essential for growth and survival.

These findings reveal that DEAF1's control of PTA expression in LNSCs is more complex than previously thought. DEAF1 can regulate PTA gene transcription directly, and control gene translation indirectly by regulating the synthesis and degradation of eIF4GII. The loss of DEAF1 function during the progression of T1D or NOD disease may affect PTA presentation on LNSCs, as shown in Figure 7. Splicing of *Deaf1* down-regulates *Eif4g3* and eIF4G3 expression, which results in reduced translation of genes including *Anpep*. Diminished aminopeptidase N expression may impact the processing of antigens on MHC class II and affect T cell activation, thereby allowing self-reactive T cells to escape deletion during T1D or NOD disease.

Materials and methods

Mice

Female NOD/LtJ (NOD), NOD.B10Sn-*H2^b*/J (NOD.B10), and BALB/c mice were purchased from Jackson Laboratories, and *Deaf1*-KO and WT (BALB/c) littermate control mice were bred at the Stanford School of Medicine Animal facility (Yip et al., 2009). All mice were maintained under pathogen-free conditions according to institutional guidelines under approved protocols in the Stanford Medical Center's Department of Comparative Medicine (Stanford, CA, USA).

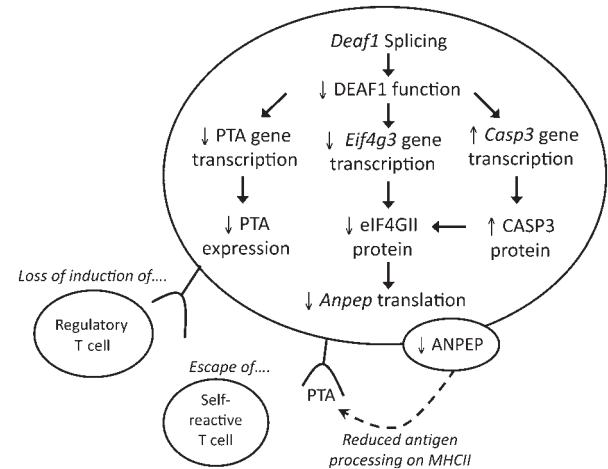


Figure 7 A model showing how *Deaf1* splicing may affect PTA expression on LNSCs. Inflammation in the PLNs of 12-week-old NOD mice (or T1D patients) can induce the splicing of *Deaf1*, which leads to the loss of DEAF1 function. This results in reduced expression of PTAs and *Eif4g3*/eIF4GII, and increased expression of *Casp3*/CASP3. Diminished eIF4GII levels lead to the loss of *Anpep* translation, which can affect antigen presentation on MHC II. Together, these changes could impact T cell engagement with LNSCs, and contribute to the escape of self-reactive T cells or prevent the induction of autoantigen-specific regulatory T cells.

Cells

The PCRC-1 (gp38⁺CD31[−]) LNSC line, T cells, B cells, and LN stromal element-enriched cells were prepared as previously described (Yip et al., 2009). The isolation of LNSC subsets was adapted from several protocols (Lee et al., 2007; Link et al., 2007; Gardner et al., 2008; Cohen et al., 2010; Fletcher et al., 2010) and is described in the Supplementary material.

Human PLN and spleen samples

Transplant grade quality PLNs and spleen of T1D patients and normal controls were obtained through the JDRF network for Pancreatic Organ Donors with Diabetes (nPOD). Human subjects approval were provided by nPOD. Sample information is available at nPOD (<http://www.jdrfnpod.org/online-pathology.php>) and in Supplementary Table S2.

Microarray analysis of gene expression in the PLNs of Deaf1-KO mice

Tissues from *Deaf1*-KO mice (4, 12, and 30-week old) and age-matched control mice were homogenized in Trizol Reagent (for the 4-week-old group: two *Deaf1*-KO and two WT controls were used, for the 12- and 30-week-old groups: three *Deaf1*-KO and three WT controls were used). RNA was extracted and microarray was performed using the Whole Mouse Genome Microarray Kit, 4 × 44K two-color arrays (Agilent Technologies), as previously described (Yip et al., 2009). Gene expression was measured in the PLNs of each individual *Deaf1*-KO animal against a pool of PLN from age-matched WT controls. Data were processed with Feature Extraction Software (Agilent Technologies), and analyzed using GeneSpring GX 11.5 Software (Agilent Technologies). Samples were filtered for detected entities, and for entities that were up- or down-regulated by 2-folds or more in all animals of a particular group compared with age-matched controls. Because of the limited number of *Deaf1*-KO individuals in each age group ($n = 2-3$), statistics could not be performed to identify genes that were significantly down-regulated in each age group. qPCR was used to accurately quantify any genes of interest. All microarray data have been submitted to the Gene Expression Omnibus (GEO) Database at NCBI (GEO series accession number: GSE29153).

Quantitative real-time RT-PCR in tissue, cells, and polysome fractions

Total RNA was extracted using Trizol reagent and the Qiagen RNeasy mini kit or micro kit, as previously described (Yip et al., 2009). First-strand cDNA was generated using the iScript cDNA synthesis kit (Biorad). Quantitative PCR was performed to measure mouse *Eif4g3*, *Eif4g1*, *Casp3*, *Deaf1*, *Ins2*, *Fgb*, *Ela*, *Ppy*, *Tyr*, *Ambp*, *Gapdh*, and *Actb* mRNA levels, and human *EIF4G3*, *EIF4G1*, *CASP3* and *ACTB*, and *GAPDH* mRNA levels. cDNA was preamplified using the Taqman PreAmp Mastermix (Applied Biosystems) prior to QPCR for *Ins2* and for gene expression measured in polysome fractions and LNSC subsets. For all other experiments, cDNA was not pre-amplified. qPCR assays were performed using the 7900HT Fast Real Time PCR System (Applied Biosystems), Taqman Gene Expression Arrays (Applied Biosystems), and SsoFast Probes Supermix (Biorad). For human *CASP3* measurements, Quantitect primers (Qiagen) and SsoFast EvaGreen Supermix (Biorad) were used. The comparative Ct

method for relative quantification ($\Delta\Delta Ct$) was used, and expression was normalized with housekeeping gene expression.

Silencing of Deaf1 and Eif4g3 by siRNA

Deaf1 (siRNA ID: s79402), *Eif4g3* (siRNA ID: s232114), and control (siRNA ID: AM4611) siRNA constructs were purchased from Ambion (Austin). PCRC-1 cells were grown in 12-well plates, and allowed to reach $\geq 80\%$ confluency prior to transfection. Cells were transfected with 40 pmol of siRNA using Lipofectimine 2000 (Invitrogen). For the polysome analysis experiments, PCRC-1 cells were grown in 10 cm plates, allowed to reach $\geq 80\%$ confluency and then transfected with 400 pmol of control or *Eif4g3* siRNA using Lipofectamine 2000.

SDS-PAGE and immunoblotting

Whole-cell extracts were prepared by lysing cells in MPER Mammalian Protein Extraction reagent (Thermo Scientific) containing 1 × HALT protease inhibitor cocktail (Thermo Scientific). Samples were prepared in Laemmli Sample buffer containing β -mercaptoethanol (Biorad). Proteins from polysome fractions were extracted as described below.

The following antibodies were used: rabbit polyclonal to eIF4G (Cell Signaling, #2469, at 1:1000), Rabbit polyclonal to Caspase 3 (Cell Signaling, #9662, at 1:1000), Rabbit monoclonal to β -actin conjugated to HRP (Cell Signaling, #13E5, 1:1000), Rabbit polyclonal to GAPDH (Abcam, Ab4985, at 1:2500), anti-rabbit HRP secondary antibody (Zymed, at 1:15000). Densitometric analysis was performed with ImageJ analysis software (version 1.43, NIH, USA). Protein expression was normalized with β -actin expression.

Polysome analysis: RNA isolation, protein precipitation, and microarray analysis

siRNA-transfected PCRC-1 cells were processed for polysome analysis 48 h after transfection based on previously published methods (Wehner et al., 2010), with the following modification: Cell lysates were layered on a 10%–60% continuous sucrose gradient (150 mM KCl, 15 mM Tris-HCl, pH 7.5, 5 mM MgCl₂, and 100 μ g/ml cycloheximide) and centrifuged (210000 × *g* for 165 min at 4°C). Proteins were precipitated from fractions (100 μ l) with 250 μ g/ml heparin, 72.5 mM NaCl, and 400 μ l methanol, resuspended in 8 M urea in 10 mM Tris-HCl (pH 8), and analyzed by immunoblotting.

RNA was isolated by acid phenol/chloroform extraction and analyzed using the Agilent 2100 Bioanalyzer and the RNA 6000 Nano Reagent Kit (Agilent). For the heavy polysome fractions, equal amounts of total RNA from fractions 10–13 were pooled together to give a final concentration of 20 ng/ μ l and used for microarray analysis. Four individual polysome analysis experiments were performed. Microarrays were performed for all four experiments as described above. Analysis was performed using Genespring 11.5. Only entities that were detected in at least two of the four samples in both the whole-cell lysates and heavy polysome fractions were included in the analysis. Data were filtered for genes that were down-regulated by ≥ 2 -fold in at least three out of the four samples. Data sets were submitted to the GEO Database (GEO series accession number: GSE39408). For qPCR, pooled RNA (200 ng) from the polysome fractions were reverse transcribed, and pre-amplified. For comparison of gene expression

within a particular fraction, *Actb* expression was used as the housekeeping gene. For comparison of expression between top, light, and heavy fractions, expression was not normalized with *Actb* since *Actb* levels differed significantly between fractions.

Caspase 3 activity

Caspase 3 activity was assessed in PCRC-1 cells 18 and 24 h after *Deaf1* silencing using the Caspase-3 Fluorometric Assay (R&D systems) and the Flexstation II Fluorescence plate reader (Molecular Devices) according to manufacturer's instructions.

Statistical analysis

Statistical analyses were performed using two-tailed unpaired Student's *t*-test or the two-tailed Mann–Whitney test, where appropriate. $P \leq 0.05$ was considered significant. Statistics were performed using Prism 5 (GraphPad Software Inc.).

Supplementary material

Supplementary material is available at *Journal of Molecular Cell Biology* online.

Acknowledgements

This research was performed with the support of the Network for Pancreatic Organ Donors with Diabetes (nPOD), a collaborative type 1 diabetes research project sponsored by the JDRF. Organ Procurement Organizations (OPO) partnering with nPOD to provide research resources are listed at www.jdrfnpod.org/our-partners.php. We thank Karla Kirkegaard for fostering communication between the Fathman and Sarnow labs.

Funding

This work was supported by the National Institutes of Health (DK078123 and AI083628 to C.G.F.), the Juvenile Diabetes Research Foundation (L.Y. and R.J.C.), the American Diabetes Association (L.Y.), and the Damon Runyon Cancer Foundation (C.T.P.).

Conflict of interest: none declared.

References

- Abbott, C.M., and Proud, C.G. (2004). Translation factors: in sickness and in health. *Trends Biochem. Sci.* 29, 25–31.
- Anderson, M.S., Venanzi, E.S., Klein, L., et al. (2002). Projection of an immunological self shadow within the thymus by the aire protein. *Science* 298, 1395–1401.
- Bagri, A., Marin, O., Plump, A.S., et al. (2002). Slit proteins prevent midline crossing and determine the dorsoventral position of major axonal pathways in the mammalian forebrain. *Neuron* 33, 233–248.
- Baker, C.C., and Fuller, M.T. (2007). Translational control of meiotic cell cycle progression and spermatid differentiation in male germ cells by a novel eIF4G homolog. *Development* 134, 2863–2869.
- Caron, S., Charon, M., Cramer, E., et al. (2004). Selective modification of eukaryotic initiation factor 4F (eIF4F) at the onset of cell differentiation: recruitment of eIF4GII and long-lasting phosphorylation of eIF4E. *Mol. Cell. Biol.* 24, 4920–4928.
- Castello, A., Alvarez, E., and Carrasco, L. (2006). Differential cleavage of eIF4GI and eIF4GII in mammalian cells. Effects on translation. *J. Biol. Chem.* 281, 33206–33216.
- Clarkson, B.K., Gilbert, W.V., and Doudna, J.A. (2010). Functional overlap between eIF4G isoforms in *Saccharomyces cerevisiae*. *PLoS One* 5, e9114.
- Cohen, J.N., Guidi, C.J., Tewalt, E.F., et al. (2010). Lymph node-resident lymphatic endothelial cells mediate peripheral tolerance via Aire-independent direct antigen presentation. *J. Exp. Med.* 207, 681–688.
- Coldwell, M.J., and Morley, S.J. (2006). Specific isoforms of translation initiation factor 4GI show differences in translational activity. *Mol. Cell. Biol.* 26, 8448–8460.
- Fletcher, A.L., Lukacs-Kornek, V., Reynoso, E.D., et al. (2010). Lymph node fibroblastic reticular cells directly present peripheral tissue antigen under steady-state and inflammatory conditions. *J. Exp. Med.* 207, 689–697.
- Fletcher, A.L., Malhotra, D., and Turley, S.J. (2011). Lymph node stroma broaden the peripheral tolerance paradigm. *Trends Immunol.* 32, 12–18.
- Gabrilovac, J., Cupic, B., Zivkovic, E., et al. (2011). Expression, regulation and functional activities of aminopeptidase N (EC 3.4.11.2; APN; CD13) on murine macrophage J774 cell line. *Immunobiology* 216, 132–144.
- Gagnerault, M.C., Luan, J.J., Lotton, C., et al. (2002). Pancreatic lymph nodes are required for priming of beta cell reactive T cells in NOD mice. *J. Exp. Med.* 196, 369–377.
- Gardner, J.M., Devoss, J.J., Friedman, R.S., et al. (2008). Deletional tolerance mediated by extrathymic Aire-expressing cells. *Science* 321, 843–847.
- Gingras, A.C., Raught, B., and Sonenberg, N. (1999). eIF4 initiation factors: effectors of mRNA recruitment to ribosomes and regulators of translation. *Annu. Rev. Biochem.* 68, 913–963.
- Gradi, A., Imataka, H., Svitkin, Y.V., et al. (1998a). A novel functional human eukaryotic translation initiation factor 4G. *Mol. Cell. Biol.* 18, 334–342.
- Gradi, A., Svitkin, Y.V., Imataka, H., et al. (1998b). Proteolysis of human eukaryotic translation initiation factor eIF4GII, but not eIF4GI, coincides with the shutoff of host protein synthesis after poliovirus infection. *Proc. Natl. Acad. Sci. USA* 95, 11089–11094.
- Hahm, K., Sum, E.Y., Fujiwara, Y., et al. (2004). Defective neural tube closure and anteroposterior patterning in mice lacking the LIM protein LMO4 or its interacting partner Deaf-1. *Mol. Cell. Biol.* 24, 2074–2082.
- Hansen, A.S., Noren, O., Sjostrom, H., et al. (1993). A mouse aminopeptidase N is a marker for antigen-presenting cells and appears to be co-expressed with major histocompatibility complex class II molecules. *Eur. J. Immunol.* 23, 2358–2364.
- Huggenvik, J.I., Michelson, R.J., Collard, M.W., et al. (1998). Characterization of a nuclear deformed epidermal autoregulatory factor-1 (DEAF-1)-related (NUDR) transcriptional regulator protein. *Mol. Endocrinol.* 12, 1619–1639.
- Kataki, T., Hara, T., Sugai, M., et al. (2004). Lymph node fibroblastic reticular cells construct the stromal reticulum via contact with lymphocytes. *J. Exp. Med.* 200, 783–795.
- Kimball, S.R., Jefferson, L.S., Fadden, P., et al. (1996). Insulin and diabetes cause reciprocal changes in the association of eIF-4E and PHAS-I in rat skeletal muscle. *Am. J. Physiol.* 270, C705–C709.
- Larsen, S.L., Pedersen, L.O., Buus, S., et al. (1996). T cell responses affected by aminopeptidase N (CD13)-mediated trimming of major histocompatibility complex class II-bound peptides. *J. Exp. Med.* 184, 183–189.
- Lee, J.W., Epardaud, M., Sun, J., et al. (2007). Peripheral antigen display by lymph node stroma promotes T cell tolerance to intestinal self. *Nat. Immunol.* 8, 181–190.
- Leenen, P.J., Melis, M., Kraal, G., et al. (1992). The monoclonal antibody ER-BMDM1 recognizes a macrophage and dendritic cell differentiation antigen with aminopeptidase activity. *Eur. J. Immunol.* 22, 1567–1572.
- Liadis, N., Murakami, K., Eweida, M., et al. (2005). Caspase-3-dependent beta-cell apoptosis in the initiation of autoimmune diabetes mellitus. *Mol. Cell. Biol.* 25, 3620–3629.
- Link, A., Vogt, T.K., Favre, S., et al. (2007). Fibroblastic reticular cells in lymph nodes regulate the homeostasis of naive T cells. *Nat. Immunol.* 8, 1255–1265.
- Lynch, S.A. (2005). Non-multifactorial neural tube defects. *Am. J. Med. Genet. C Semin. Med. Genet.* 135C, 69–76.
- Marissen, W.E., Gradi, A., Sonenberg, N., et al. (2000). Cleavage of eukaryotic translation initiation factor 4GII correlates with translation inhibition during apoptosis. *Cell. Death Differ.* 7, 1234–1243.
- Marissen, W.E., and Lloyd, R.E. (1998). Eukaryotic translation initiation factor 4G is targeted for proteolytic cleavage by caspase 3 during inhibition of translation in apoptotic cells. *Mol. Cell. Biol.* 18, 7565–7574.
- Meric, F., and Hunt, K.K. (2002). Translation initiation in cancer: a novel target for therapy. *Mol. Cancer Ther.* 1, 971–979.

- Michelson, R.J., Collard, M.W., Ziemba, A.J., et al. (1999). Nuclear DEAF-1-related (NUDR) protein contains a novel DNA binding domain and represses transcription of the heterogeneous nuclear ribonucleoprotein A2/B1 promoter. *J. Biol. Chem.* 274, 30510–30519.
- Nichols, L.A., Chen, Y., Colella, T.A., et al. (2007). Deletional self-tolerance to a melanocyte/melanoma antigen derived from tyrosinase is mediated by a radio-resistant cell in peripheral and mesenteric lymph nodes. *J. Immunol.* 179, 993–1003.
- Sun, F., Palmer, K., and Handel, M.A. (2010). Mutation of Eif4g3, encoding a eukaryotic translation initiation factor, causes male infertility and meiotic arrest of mouse spermatocytes. *Development* 137, 1699–1707.
- Wehner, K.A., Schutz, S., and Sarnow, P. (2010). OGFOD1, a novel modulator of eukaryotic translation initiation factor 2alpha phosphorylation and the cellular response to stress. *Mol. Cell. Biol.* 30, 2006–2016.
- Yip, L., Su, L., Sheng, D., et al. (2009). Deaf1 isoforms control the expression of genes encoding peripheral tissue antigens in the pancreatic lymph nodes during type 1 diabetes. *Nat. Immunol.* 10, 1026–1033.